ELSEVIER

Journal of Nuclear Materials 296 (2001) 210–218

journal of nuclear materials

www.elsevier.com/locate/jnucmat

Section 4. Liquid metal corrosion and embrittlement

Thermal gradient mass transfer of type 316L stainless steel and alloy 718 in flowing mercury

S.J. Pawel *, J.R. DiStefano, E.T. Manneschmidt

Metals and Ceramics Division, Oak Ridge National Laboratory, P.O. Box 2008, Oak Ridge, TN 37831-6156 USA

Abstract

Thermal convection loops (TCLs) fabricated from 316L stainless steel (SS) and containing mercury and a variety of 316L coupons representing variable surface conditions and heat treatments have been operated continuously for periods up to 5000 h. In each case, the maximum TCL temperature was about 305°C, the minimum temperature about 240°C, and the Hg velocity was constant at either 1.2 m/min or 5 m/min, depending on the TCL cross-section diameter. Wetting of 316L by Hg was somewhat sporadic and inconsistent, and was generally encouraged by steam cleaning and/or gold-coating of specimens prior to testing as well as relatively high exposure temperatures. Interaction of 316L and Hg was observed to generate a porous surface layer substantially depleted of Ni and Cr which resulted in transformation to ferrite, but the maximum penetration detected for all of the test conditions corresponded to only about 60–70 μm/yr, with far less penetration for most exposures. In limited testing, alloy 718 was found more resistant to wetting/attack than 316L.

1. Introduction

The spallation neutron source (SNS) will generate neutrons via interaction of a 1.0 GeV proton beam with a liquid mercury target. Type 316L/316LN austenitic stainless steel (SS) has been selected as the primary target containment material [1] based on a favorable combination of several factors, including resistance to corrosion by Hg, well-characterized behavior in a neutron radiation environment, and the absence of a significant ductile–brittle transition temperature such as that found in irradiated ferritic stainless steels.

The energy deposited in the Hg target by the proton beam (design basis is presently 2 MW) will be dissipated by circulating the mercury through standard heat exchangers. Various fluid dynamics computations and simulations of conditions expected in the target predict maximum (localized) bulk mercury temperatures on the order of 150°C with nominal temperatures closer to 100–120°C. The mercury temperature at the target inlet is expected to be near ambient.

As a result of the temperature gradient in flowing Hg, thermal gradient mass transfer effects are being investigated. In this form of corrosion, dissolution of the container material by the liquid in relatively high temperature (high solubility) regions is accompanied by deposition of solute in relatively colder regions [2]. Since some corrosion product is removed during each temperature cycle, dissolution in the high temperature region is not limited by system equilibrium (saturation considerations) and attack is potentially accelerated over what would be experienced in an isothermal/stagnant system. In addition to accelerated dissolution, deposition of solute material in the cold regions has been known to cause flow disruptions and can even plug flow paths in liquid metal loops [3]. Among the major alloying elements of stainless steels, nickel is expected to have the highest solubility in mercury [4] at SNS operating temperatures, and therefore this element may be the most susceptible to mass transfer.

At the expected SNS operating temperatures, pure mercury does not readily chemically wet 316/316L stainless steel. Without chemical wetting (characterized macroscopically by a low contact angle with an Hg

* Corresponding author. Tel.: +1-865 574 5138; fax: +1-865 241 0215.

E-mail address: pawelsj@ornl.gov (S.J. Pawel).

0022-3115/01/$ - see front matter
PII: S0022-3115(01)00520-7

droplet), any potential corrosion process is inhibited. However, mercury can sometimes be made to wet 316/316L in air or vacuum by raising the temperature to 225–275°C [5]. Despite the relatively low expected operating temperatures of the SNS, chemical wetting of containment surfaces may be encouraged in the SNS target by a combination of several factors:

1. the presence of thermal hot spots,
2. radiation damage in the presence of Hg, and
3. generation of fresh (oxide-free) surfaces that result from potential cavitation and thermal shock/fatigue loading to which the target containment material will be exposed.

Clearly, to examine potential 'worst case' mass transfer corrosion, it is desirable to develop wetting in the tests with flowing mercury. Therefore, the thermal convection loop (TCL) tests in this program utilized relatively high peak temperatures (near 300°C) to achieve at least some amount of wetting. In addition, small amounts of Ga (up to 1000 wppm) were added to the Hg in some tests in an attempt to increase the tendency of the liquid metal to wet the loop containment and coupons. Gallium was chosen as an additive because it is an aggressive metal that wets many materials and because it has some solubility in Hg (even at room temperature). This document describes the operation of these TCLs and the results obtained.

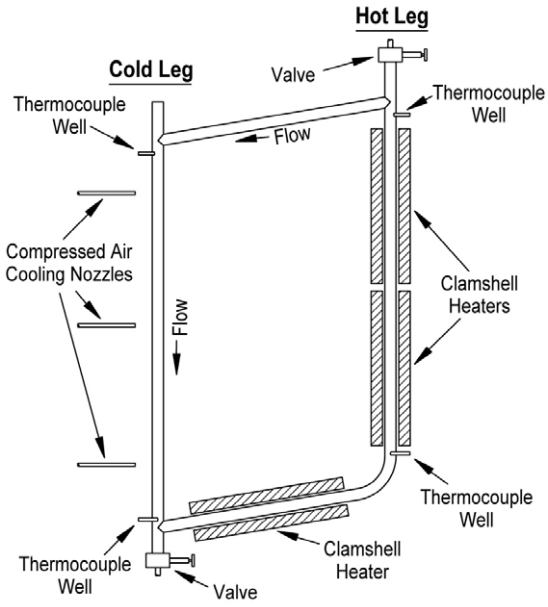

Fig. 1. Schematic of the TCL design. The distance between thermocouple wells on each vertical section is about 0.7 m and the vertical sections are separated by about 0.5 m.

2. Experimental

2.1. Loop fabrication

A schematic of the TCL design is shown in Fig. 1. For the study of 316L SS, each TCL was fabricated of mill annealed 316L SS seamless tubing (25.4 mm ID, 1.8 mm wall) with the composition shown in Table 1. The thermocouple wells, which protruded about 10 mm into the flow channel, were also seamless, mill annealed 316L SS tubing (6.4 mm OD, 0.7 mm wall). Valves and other metallic accessories (connectors, transfer lines, etc.) were 316 or 316L stainless steel. For study of alloy 718, identical TCLs were fabricated except that the major tubing components were all seamless, mill annealed (not hardened) alloy 718.

Each TCL contained a chain of specimens in the heated and cooled vertical sections (typically termed the 'hot leg' and 'cold leg,' respectively). Each specimen chain consisted of 32 specimens, nearly all of which were thin rectangular coupons with dimensions as shown in Fig. 2. In a few cases, a limited number of miniature tensile specimens made from the same heat of material as the rectangular coupons were also included on the chain. The specimens were joined together with a continuous wire (about 0.4 mm diameter, 316L or alloy 718) via the holes in the corners/ends of each specimen. The end of each wire was welded to the bottom of the respective vertical sections to keep the chains from floating to the top of the Hg, and to keep the coupons positioned such that the top and bottom of the chain corresponded approximately to the thermocouple well positions in each leg. To minimize specimen movement relative to each other and facilitate close spacing, adjacent rectangular coupons were interlocked via the small notch at each end of the specimen; thus, alternating coupons were turned 90° relative to each other.

The 'standard' coupon for the 316L SS studies was surface ground/mill annealed, and most of the 316L SS coupons exposed in the TCLs were in this condition. However, TCLs #5, 6, 7 and 8 were operated such that a number of coupons other than the 'standard' condition were also examined, including:

- polished on the large faces (1 μm alumina paste),
- oxidized (heated in air 2 h at 900°C),
- gold coated (sputter cleaned and coated 0.3 μm thick in vacuum),
- etched (40% reagent grade sulfuric acid at 70°C for six minutes),
- ion bombarded (1×10^{17} Fe/cm^2 at 30 KeV to calculated 43 dpa at surface),
- sensitized (20 h at 650°C in vacuum),
- welded (electron beam weld pad on two-thirds of specimen surface),

Table 1
Composition of TCL tubing and specimens (weight percent from mill certification)

Element	316L tubing	316L coupons	316LN coupons	718 tubing	718 coupons
Al				0.56	0.54
B				0.003	0.004
C	0.013	0.018	0.009	0.03	0.05
Co			0.16	0.13	0.40
Cr	16.75	16.10	16.31	18.39	18.13
Cu	0.30	0.29	0.23		
Fe	Balance	Balance	Balance	18.52	18.35
Mn	1.84	1.73	1.75	0.06	0.21
Mo	2.12	2.15	2.07	2.95	3.01
N	0.046	0.030	0.11		
Nb	0.17			5.09	5.07
Ni	10.19	10.10	10.20	53.14	52.70
P	0.028	0.028	0.029	0.010	0.005
S	0.014	0.005	0.002	0.001	0.002
Si	0.34	0.50	0.39	0.12	0.13
Ti				0.95	1.06

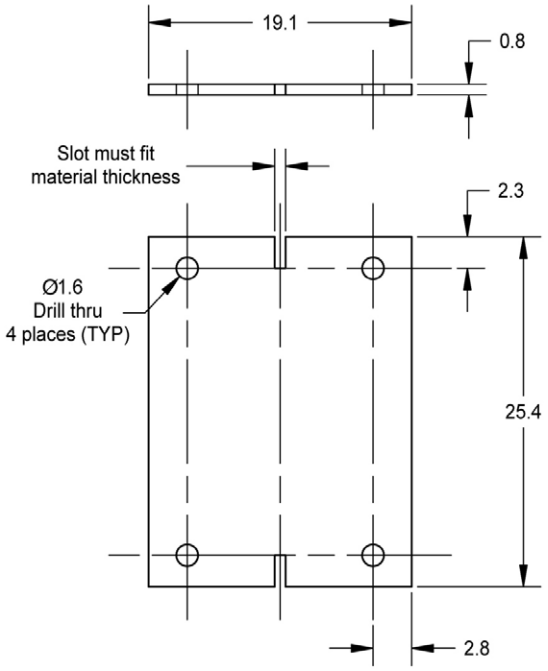

Fig. 2. Dimensions (given in mm) of rectangular coupons.

- 316LN (mill annealed, but nitrogen bearing composition).

The specimens in each chain were individually numbered, cleaned ultrasonically in acetone, and weighed (before and after each 'treatment,' if any) prior to assembly of the chain. All specimens were handled with gloves and tweezers during the stacking and wiring activities. Other details of the experiments, specimens, and arrangement appear in [6–8].

2.2. Filling with mercury

Each TCL was alternately evacuated (internal pressure of a few microns of Hg) and filled with helium several times. Subsequently, the loop was evacuated and filled with Hg from the reservoir at the top (the ullage of which was also evacuated/purged with helium). Approximately one atmosphere of helium was used as a cover gas for the Hg in the loop. The loop was warmed to near operating temperature and the excess Hg (expanded above fill line at room temperature) was drained through a side arm of the loop.

Virgin mercury from the same batch was used for all these experiments. Standard chemical analysis of representative samples indicated the Hg was quite pure, containing only about 85 ppb Ag and 100 ppb Si above detection limits. Immediately prior to use in the loops, the Hg was 'filtered' through cheesecloth to remove the small amount of residual debris (oxides) floating on the surface of the Hg.

2.3. Loop operation

The heat-up and operation of the TCLs was essentially identical for each experiment. Two clamshell-type furnaces heated the vertical leg and one heated the near-horizontal lower portion of the loop. The control temperature of the lower furnace was kept somewhat below the temperature of those on the vertical hot leg to maintain the desired mercury flow pattern. The vertical section of each cold leg was cooled by compressed air delivered from three roughly equi-spaced copper tubes with outlets placed close to the outer loop surface and an array of small fans providing air movement across the entire cold leg. During initial operation (the first few days), minor adjustments were made to the furnace

Table 2
Typical temperature at each 'corner' of the TCLs. For an individual TCL, the temperatures nominally experience a ±2°C drift over the duration of an experiment

Position	Temperature (°C)
Top of hot leg	305
Top of cold leg	280
Bottom of cold leg	242
Bottom of hot leg	268
Maximum gradient	63

temperature and airflow, after which the temperature at each thermocouple well position and the mercury flow rate became quite stable. The temperature at each location varied only by about ±2°C over the entire duration of the experiments (up to 5000 h of uninterrupted operation). Table 2 indicates the nominal temperatures at each thermowell for these TCLs.

The flow rate of the mercury inside the loop was determined via a localized 'temperature spike' test. In this test, a propane torch was used to heat a small area in the middle of the roughly horizontal section at the top of the loop for about 15 s. The time required for the resultant temperature 'spike' to reach each thermocouple in sequence around the loop along with the distance between thermocouples was used to estimate the velocity of the mercury. The mercury flow rate was found to be approximately constant at 1.2 m/min in each loop over the duration of the experiment. In one set of experiments, the Hg velocity in the TCL was locally increased to about 5 m/min by inserting a venturi-shaped reduced section near the top of the hot leg. However, the average velocity in the TCL with the restricted section remained near 1.2 m/min.

Other details of the experimental arrangement, in particular the cleaning steps prior to assembly and just before filling with Hg, the addition of Ga (to 1000 wppm, as a potential aid to wetting) in some experiments, and one loop which received a pre-soak in Hg at 320°C prior to operation, are provided in [6–8]. Table 3 summarizes the TCL test matrix.

3. Results and discussion

3.1. Loops #1 and #2

Both of these 316L SS TCLs were operated without interruption for about 5000 h each. One loop circulated pure Hg and in the other 1000 wppm Ga was added to the Hg. Detailed results are given in [6]; only key results are summarized here. However, one factor worth noting is that the loop internals (tube walls and coupons) were steam cleaned immediately prior to filling with Hg.

Weight change as a function of position (temperature) for the coupons exposed to pure Hg for 5000 h in loop #1 is shown in Fig. 3. Temperature at each coupon position was estimated by assuming a linear variation with distance between thermocouples at the top and bottom of each coupon chain. The maximum weight loss (coupon at the top of the hot leg, 305°C) corresponds to a uniform general corrosion rate of about 3.8 μm/yr for the duration of the loop exposure.

Fig. 4 is representative of the cross-section of the coupon from the top of the hot leg (maximum weight change). In the as-polished condition, it reveals a shallow 'reaction zone' at the specimen surface which appears significantly altered from the composition/structure of the base material. The affected region is

Table 3
Summary of general test materials and conditions for the thermal convection loops in this investigation

Loop	Fluid	Test material	Coupon condition	Exposure time (h)	Special feature (s)
1	Hg	316L	Mill-annealed + surface-ground	5000	Steam cleaned after assembly
2	Hg + Ga	316L	Mill-annealed + surface-ground	5000	Steam cleaned after assembly
3	Hg	718	Mill-annealed + surface-ground	5000	
4	Hg + Ga	718	Mill-annealed + surface-ground	5000	
5	Hg	316L + 316LN	Wide variety of surface and heat treatments	2000	Hot and cold leg soaked in Hg at 320°C
6	Hg	316L + 316LN	Wide variety of surface and heat treatments	2000	
7	Hg	316L	Wide variety of surface and heat treatments	2000	Reduced section in hot leg to increase local velocity
8	Hg	316L	Wide variety of surface and heat treatments	2000	Reduced section in hot leg to increase local velocity and steam cleaned

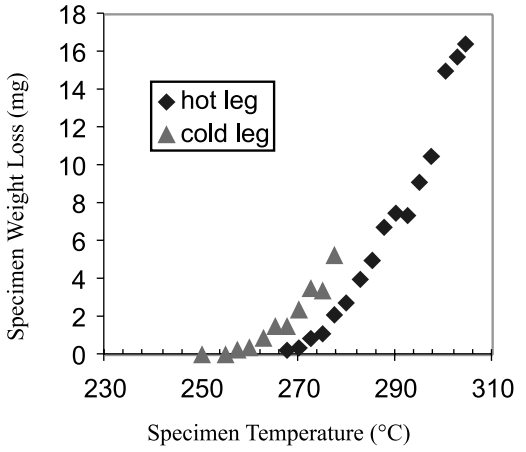

Fig. 3. Specimen weight loss as a function of temperature (position) after 5000 h exposure in loop #1.

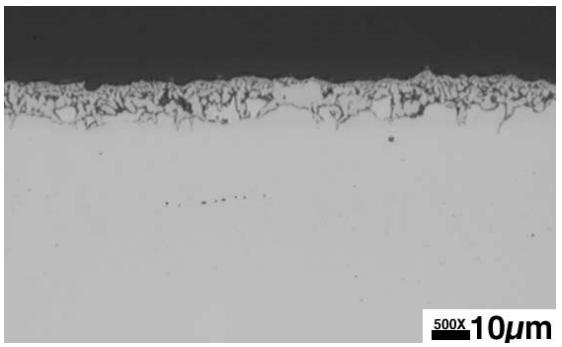

Fig. 4. As-polished cross-section of 316L specimen from the top of the hot leg (305°C) in loop #1 for 5000 h.

relatively uniform in appearance (porosity approximately constant at about 23% based on area mapping) and depth (average is 9–10 μm, maximum is 12 μm) on all exposed surfaces of the coupon. When etched (Fig. 5),

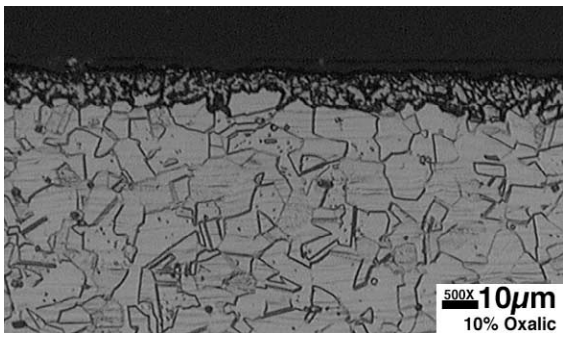

Fig. 5. Etched (electrolytic 10% oxalic acid) cross-section of 316L specimen shown in Fig. 4.

the reaction zone appears to advance preferentially along grain boundaries. Similar attack patterns were noted for other coupons with measurable weight loss (those exposed above about 255°C) except that, corresponding to lesser weight change, the corroded layer was thinner in proportion to the weight change. For coupons exposed below about 255°C, no reaction zone was detected and no change in the original surface roughness of the coupon was apparent.

Microprobe chemical analysis was performed at a number of locations across the corroded region into the base material. A representative scan is shown in Fig. 6 for the coupon revealing the maximum weight change. The corroded region was found to be completely depleted of Ni and about 70% depleted of Cr. While present in a smaller overall amount, the Mo concentration did not appear to be significantly different from that of the bulk material. Consistent with the change in composition, the surface layer was found to be ferritic (magnetic). Similar porous layers associated with selective dissolution of Ni and Cr have been observed for type 316 SS in Li [9,10] and Pb–17%Li [11,12].

The representative data also reveal that the composition gradient between the depleted surface material and the adjacent substrate is very steep. In this case, the scans compare elemental concentrations just barely on the liquid side of the reaction interface (spot centered

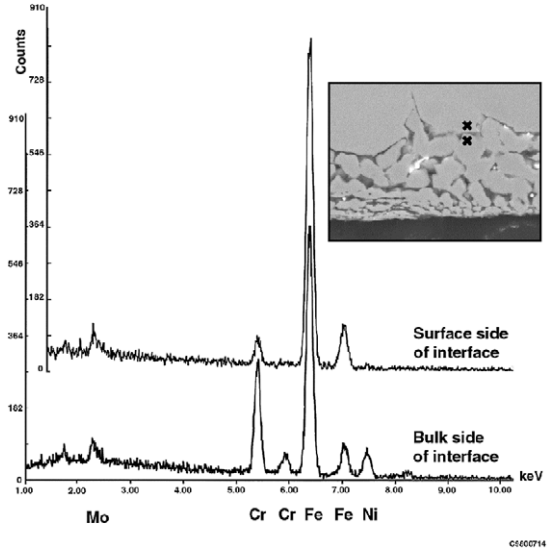

Fig. 6. Representative microprobe data from 316L specimen from the top of the hot leg (305°C) in loop #1. Elements associated with major peaks identified along *x*-axis. Note that the peak associated with Ni is absent and the peaks associated with Cr are significantly reduced from the scan on corroded material. Surface side analysis spot centered about 6.8 μm from the exposed surface while the bulk side analysis spot is at a depth of about 8.3 μm.

6.8 μm from the outer surface) with material just barely on the bulk side of the interface (spot centered 8.3 μm from the outer surface). Further, microprobe analyses revealed the composition of the porous material to be the same everywhere, and the composition of the material just barely on the bulk side of the interface matched that of the stainless steel very far removed from the interface.

One concern for the SNS target is the possible effect of radiation (high dpa) in austenitic stainless steels on radiation-enhanced diffusion of nickel [13,14]. Potentially, this factor could increase availability/leaching of Ni into the Hg in the actual SNS target compared to the TCL exposures. In addition, other factors – such as the influence of radiation and radiation products on wetting and the mechanism by which Ni is rejected from solution in the Hg – could also play important roles.

Interestingly, the TCL walls (even at the top of the hot leg) were apparently not wetted by Hg and were observed metallographically to be absent of attack. This is somewhat confounding in light of the fact that the loop walls act as a heat transfer surface and are therefore at a slightly higher temperature (in the hot leg) than the corresponding coupons inside the loop. Presently, it is suspected that some aspect of the surface condition (in particular, tube cleanliness or lack thereof) may be responsible for a residual film that inhibited wetting and interaction with Hg.

Using the treatment of Epstein [2] and extending it similar to the manner of Tortorelli and DeVan [9] and Holman [15], an attempt was made to use the mass loss as a function of temperature data to derive the activation energy for the rate controlling step of the corrosion/leaching process. (The reader is referred to [6] for details.) In each case, the activation energy for the process was found to be on the order of about 3 kJ/mol. Even in consideration of the potential errors that may be introduced by the limited amount of data, the activation energy determined from the data for loop #1 is so low that solid-state diffusion (solution rate limited corrosion) does not appear to be a factor. Rather, the very low activation energy suggests that a reaction such as a phase transformation or liquid-state diffusion is controlling.

One possibility for liquid-state diffusion control is the mechanism in which solute atoms (Ni and Cr) rapidly enter the liquid from the ferrite and tend to saturate the liquid boundary layer. The rate at which the process proceeds is controlled by the rate solute atoms can diffuse from the boundary layer to the bulk liquid. At the initiation of the leaching process (parent austenite or very thin ferrite layer exposed to Hg), diffusion distances in the solid are short. At longer times, the ferrite layer becomes thicker and porous, but the mercury in the pores may function to keep the diffusion distances short for transport of Ni and Cr to the liquid. However, at some point in the process, the mercury in the pores may become sufficiently occluded from the bulk mercury that bulk velocity has only minimal influence on the boundary layer. In such a case, a low activation energy for the process would be expected but the process would be expected to remain relatively insensitive to bulk velocity.

Also of interest in loop #1 is the fact that no surfaces (coupons or tube internals) experienced deposits or weight gains. When the TCL was drained after the test, a small amount of green/gray powder was found floating on the surface of the last Hg to drain from the loop. The material was found to be only partially crystalline and to contain a substantial amount of NiO and $(Cr,Fe)_2O_3$. (The source of Ni and Cr likely to be material leached from hot leg coupons.) If wetting had developed in the colder portions of the TCL, this material presumably would have deposited on cold leg surfaces/coupons. However, the absence of wetting at low temperatures may have prohibited deposition in favor of simple precipitation from solution due to supersaturation.

Loop #2 was identical to loop #1 except that 1000 wppm Ga was added to the Hg used for the experiment. In stark contrast to the results for loop #1, no wetting by the Hg–Ga solution was observed for the exposed surfaces of loop #2 and none of the coupons exhibited any change in appearance or mass as a result of the 5000 h exposure at temperatures to 305°C. Only sporadic traces of Ga were detected on the surfaces of the coupons exposed in loop #2, so it appears unlikely that the role of Ga is related to a surface reaction/film.

3.2. Loops #3 and #4

These two 5000-h TCLs were intended to represent 'twin' loops to #1 and #2 except that the TCL material and coupons were fabricated of alloy 718, which at the time of these experiments was considered to be an alternate material selection for 316L SS for the SNS target containment. A summary of the key results appears herein; additional details can be found in [7].

Since Ni was leached from 316L SS in loop #1 and alloy 718 contains about five times the nickel of 316L SS, it was expected that alloy 718 would reveal a greater extent of attack than 316L for equivalent exposures in Hg. However, with only very minor exception, alloy 718 was not wet and therefore immune to attack in both the pure Hg loop (#3) and the Hg + 1000 wppm Ga loop (#4). Based on these results and those in [5], alloy 718 appears more resistant to wetting/attack by Hg than is 316L SS.

The reasons for the behavior of alloy 718 in the Hg loops are not clear and they may be quite complex. One possibility is that some aspect of the bulk composition (or the passive film thereon) of alloy 718 renders it less susceptible to wetting by Hg. Subtle differences in the

surface condition (cleanliness, composition of passive film, etc.) may be responsible. For example, the alloy 718 TCLs received somewhat different mechanical and chemical treatment prior to the loop operation. Perhaps the most significant difference is that, as previously noted, the 316L TCLs received a steam treatment just prior to operation where the alloy 718 loops received a mechanical and chemical cleaning prior to assembly. This difference applies most directly to the tube surfaces, but the 316L specimen chains also received steam cleaning that was not part of the alloy 718 specimen chain treatment. Further, Mo is known to enhance the stability of passive films on stainless steels in many corrosive environments, and the presence of Mo (3% in alloy 718 vs 2% in 316 SS) may be significant. Perhaps such a small composition difference seems trivial, but consider, however, that Kropowicz [16] found that 304 SS and some nickel-base alloys (all containing only trace Mo) were significantly more susceptible to liquid metal embrittlement (as revealed by low ductility in slow strain rate tests in Hg compared to air) than 316 SS containing 2% Mo.

3.3. Loops #5 and #6

The purpose of these two 316L TCLs was to examine a variety of surface conditions and heat treatments (see bullet list in Section 2.1) as they potentially influence compatibility in Hg. The tubing for each of these loops was mechanically and chemically cleaned prior to assembly in identical fashion but neither loop was given a steam treatment prior to operation. Both TCLs operated for 2000-h with pure Hg at the same conditions and temperature gradient as the other TCLs. However, rather than standard initiation of heating on the hot leg and concurrent cooling of the cold leg to establish Hg flow, the entire loop #5 was fitted with clamshell furnaces and heated to 310–320°C for about 36 h. After the soak at elevated temperature (which was intended to aid wetting of the loop surfaces and coupons), the furnaces on the cold leg and upper horizontal sections of the TCL were removed and airflow to the cold leg was initiated. Loop #6 was identical to loop #5 except that the pre-operational soak was omitted for loop #6. Other details of set-up and operation, as well as a more detailed accounting of the results, can be found in [8].

Since it is recognized that an air-formed passive film on stainless steel can be a significant barrier to chemical wetting by Hg, a small number of specimens were coated on one side with gold in an attempt to promote wetting of the stainless steel. The surfaces to be coated were sputtered in a high vacuum chamber with Ar^+ ions to remove the oxide film from the surface of the material. Next, with the specimen still in the vacuum chamber to avoid exposure to air, the coupon was rotated to a position in which a thin film of gold (approximately 0.3 μm on average) could be sputter-coated onto the exposed stainless steel surface. The gold-coated specimens could then be handled in air (removed from the chamber, added to the coupon chain, exposed to Hg) while maintaining the oxide-free nature of the surface beneath the gold. By depositing the gold in this fashion – directly onto an atomically cleaned surface rather than onto an oxide – it was expected that upon exposure, Hg would rapidly amalgamate the Au and place a large area of oxide-free stainless steel surface into direct contact with Hg.

Based upon post-test appearance, the side coated with gold experienced a significant degree of wetting compared to the uncoated side for coupons in both loops. As shown in Fig. 7, a somewhat tenacious film of Hg remained on the side formerly coated with gold, while the uncoated side was essentially devoid of visible Hg. During gold coating, the side of the coupon not being coated was supported on a circular stand. The area completely masked by the stand is evident by the relatively shiny, circular area in the center of the back of the coupon. At the extreme edges of the back, the coupon reveals no apparent wetting but some interaction with Hg has darkened the surface luster considerably. The reason for the dark coloration is not clear, but it perhaps relates to the deposit of a thin, irregular gold film which generated non-uniform interaction with Hg. However, other coupons (not associated with the gold-coating process) occasionally revealed dark discolor-

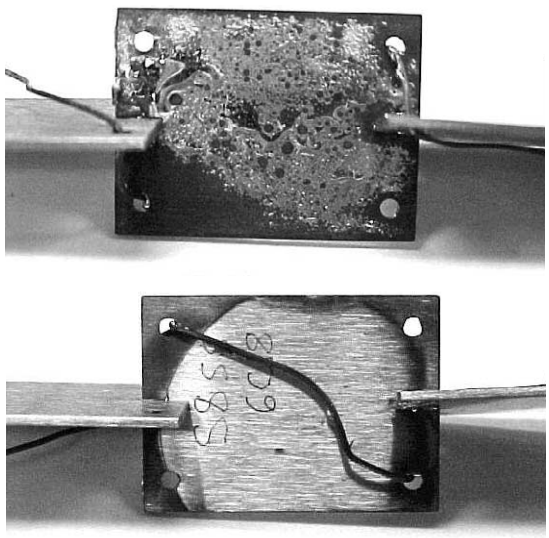

Fig. 7. Post-test appearance of specimen which was gold-coated on one side (top) and was protected from gold coating on the opposite side (bottom) by a circular support stand. The side formerly coated with gold retains no gold coloration but residual Hg clings to large portions of the surface with a low contact angle.

ation, which may suggest a mercury sulfide constituent. (Sulfur could be a trace contaminant in the Hg or in any residual air inside the loop.) After Hg was wiped from the wetted surface and the coupons were cleaned in a ultrasonic bath of acetone, the formerly wetted (gold-coated) surface revealed a dull gray luster and a slightly roughened or even lightly pitted appearance. It is interesting that any disruption of the wetted surface at room temperature, such as lightly wiping to remove bulk Hg, immediately rendered the coupon unable to 're-wet' upon dipping into ambient Hg. Even extended exposure to air with no mechanical disturbance tended to result in beading of the Hg and loss of wetting.

Post-test metallographic cross-sections of the gold-coated coupons reveal a significant increase in surface roughness on the coated side for hot- and cold-leg specimens. Fig. 8 is representative of this observation and it shows at least 15 μm of penetration into the originally uniform surface. However, relatively little of the 'porous structure' similar to that discussed in relation to Fig. 4 was observed on the coated specimens, even though the weight change on these coupons was even larger than that for previous coupons (loop #1 [6]) in which the porous surface was readily detected. Electron microprobe analysis of cross-sections of the gold-coated specimens revealed no trace of residual gold, and Ni and Cr depletion only in the small areas in which the porous structure is evident (always the side that had been coated with gold). In areas such as that depicted in Fig. 8, there was no change in composition compared to the bulk. It would appear that Hg attack was sufficiently aggressive on the gold-coated side of the coupon that small pieces of the porous surface were completely dissolved or perhaps dislodged to create the observed surface roughness and weight loss. When corrected for surface area of gold coating and total exposure time, the net weight loss of the gold-coated surfaces exceeds the maximum weight loss observed in loop #1 by about 60%. This could be due to more complete dissolution or a decrease in the time required to initiate chemical wetting and leaching. Nevertheless, the maximum extent of penetration still corresponds to only about 60–70 μm/yr (<3 mils/yr) for the conditions examined in this TCL.

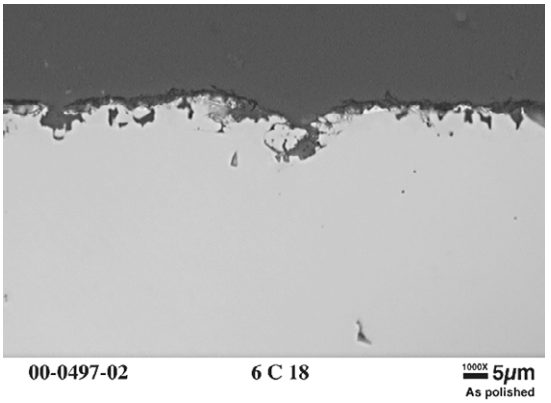

Fig. 8. As-polished cross-section of specimen surface formerly coated with gold; note surface roughness and irregular penetration.

Among all the other coupon surface conditions and heat treatments represented in this pair of tests, minor signs of residual post-test wetting were observed but no coupons revealed a weight change greater than a few percent of that observed for the gold-coated coupons. Metallographically, cross-sections of post-test coupons revealed variable degrees of attack. In the worst of these cases, regions of porous structure exhibiting leaching of Ni and Cr (similar to that shown in Fig. 4) were observed on portions of a few of the 'nominal' 316L specimens, particularly those exposed to the highest Hg temperatures. In localized areas (the extent of attack was not uniform among types of coupons or even on individual coupons), the maximum penetration observed corresponds to 8–10 μm in 2000 h. More commonly, only minor surface roughening (sporadic penetrations up to about 5 μm in 2000 h; no 'porous' structure) was observed on the post-test coupons.

No significant difference in behavior of any of the coupons or loop surfaces was observed as a result of the pre-operational soak at 310–320°C. The reader is referred to [8] for more detailed results for this pair of TCLs.

3.4. Loops #7 and #8

The purpose of these two 316L TCLs was primarily to examine the effects of increased velocity and turbulence of the Hg compared to the previous TCL tests. This was accomplished by modifying the TCL design to include a venturi-shaped section (reduced section diameter about 60% less than nominal diameter) at the top of the hot leg. Based on analytical modeling of the appropriate parameters, the flow rate in the center of the reduced section was increased from about 1.2 m/min to about 5 m/min. The two loops were identical except that one was steam cleaned just prior to operation while the other was not.

Similar to the other TCL tests, a coupon chain was deployed in each vertical leg but, because of the reduced section the coupons had to be smaller in width. The reduced section was of sufficient length that two coupons fit entirely within it – a gold-coated specimen and an otherwise nominal 316L specimen. In addition, gold-coated coupons were placed adjacent to 'nominal' coupons just below the reduced section (in the nominal velocity Hg) as well as two positions in the cold leg at nominal velocity.

Although the data analysis for the coupons and loop surfaces so exposed is not yet complete, the preliminary results suggest that velocity, at least in the range of 1–5 m/min, is not a significant factor in wetting/compatibility for 316L. The steam treatment appears to have been effective for generating macroscopic wetting, although significant wetting was observed on coupons removed from both of these TCLs. Weight changes among the coupons exposed in these loops were very minor, but metallographic evaluation is not yet complete.

4. Conclusions

Austenitic type 316L SS has been exposed to flowing Hg in thermal convection loops at temperatures up to 305°C for periods up to 5000 h. Wetting of 316L by Hg under the conditions examined was not uniform or predictable, although high temperatures, gold-coating, and steam cleaning all seemed to encourage wetting/interaction, while additions of Ga were found to be ineffective in this regard. In the cases of maximum interaction with Hg (as revealed by weight loss), a porous layer substantially depleted in Ni and Cr formed at the exposed surface, leading to transformation of the affected area to ferrite. More nominally, only slight surface roughness developed. Among all of the test exposures, heat treatments, and surface conditions examined, the maximum metallographic penetration was observed to correspond to about 60–70 μm/yr (<3 mil/yr) with much less interaction in most cases. Alloy 718 was found essentially immune to Hg under the limited set of TCL conditions to which it was exposed. The latter result is probably due to resistance to wetting rather than any fundamentally greater resistance to corrosion.

Acknowledgements

The authors would like to acknowledge the helpful role of many individuals. C.B. Herd and L.P. Smarsh fabricated the TCLs. H.F. Longmire performed the specimen metallography and E.A. Kenik performed the microprobe analysis. J.D. Hunn performed the iron implantations and H.M. Meyer and K.A. Thomas deposited the gold-coating. R.B. Ogle and S.N. Lewis provided Industrial Hygiene advice and services for controlling mercury exposures. J.H. DeVan provided many helpful discussions and insights, and along with P.F. Tortorelli provided critical review of the manuscript. F.C. Stooksbury and K A. Choudhury helped to prepare the manuscript and figures.

References

[1] L.K. Mansur, H. Ullmaier, in: Proceedings of the International Workshop on Spallation Materials Technology, CONF-9604151, Oak Ridge, TN, April 23–25, 1996.
[2] L.F. Epstein, in: F.J. Antwerpen (Ed.), Liquid Metals Technology – Part I, Chemical Engineering Progress Symposium Series, vol. 53, No. 20, 1957, p. 67.
[3] J.R. DiStefano, A review of the compatibility of containment materials with potential liquid metal targets, Oak Ridge National Laboratory Report, ORNL/TM-13056, 1995.
[4] J.R. Weeks, Corrosion 23 (1967) 98.
[5] J.R. DiStefano, S.J. Pawel, E.T. Manneschmidt, Materials compatibility studies for the spallation neutron source, Oak Ridge National Laboratory Report, ORNL/TM-13675, 1998.
[6] S.J. Pawel, J.R. DiStefano, E.T. Manneschmidt, Corrosion of Type 316L stainless steel in a mercury thermal convection loop, Oak Ridge National Laboratory Report, ORNL/TM-13754, 1999.
[7] S.J. Pawel, J.R. DiStefano, E.T. Manneschmidt, Corrosion of alloy 718 in a mercury thermal convection loop, Oak Ridge National Laboratory Report, ORNL/TM-1999/323, 1999.
[8] S.J. Pawel, J.R. DiStefano, E.T. Manneschmidt, Effect of surface condition and heat treatment on corrosion of type 316L stainless steel in a mercury thermal convection loop, Oak Ridge National Laboratory Report, ORNL/TM-2000/195, 2000.
[9] P.F. Tortorelli, J.H. DeVan, J. Nucl. Mater. 85&86 (1979) 289.
[10] P.F. Tortorelli, J.H. DeVan, J. Nucl. Mater. 122&123 (1984) 1258.
[11] P.F. Tortorelli, J.H. DeVan, J. Nucl. Mater. 141–143 (1986) 592.
[12] H. Tas et al., J. Nucl. Mater. 141–143 (1986) 571.
[13] E.A. Kenik, J. Nucl. Mater. 216 (1994) 157.
[14] S. Watanabe, J. Nucl. Mater. 232 (1996) 113.
[15] W.R. Holman, Mass transfer by high temperature liquid sodium, American Standard Report, AECU-4072, 1958.
[16] J.J. Krupowicz, in: R.D. Kane (Ed.), Slow Strain Rate Testing for the Evaluation of Environmentally Induced Cracking: Research and Engineering Applications, ASTM STP 1210, American Society for Testing and Materials, Philadelphia, PA, 1993, p. 193.